ASIAN JOURNAL OF PHARMACEUTICAL AND CLINICAL RESEARCH

INNOVARE ACADEMIC SCIENCES
Knowledge to Innovation

Vol 15, Issue 9, 2022

Online - 2455-3891
Print - 0974-2441

Research Article

USING ASPEN PLUS TO SIMULATE PHARMACEUTICAL PROCESSES – AN ASPIRIN CASE STUDY

ALISA DOUGLAS[1]*, ALI ELKAMEL[2]

[1]Integrated Biomedical Engineering and Health Sciences Program, McMaster University, Hamilton, Canada. [2]Department of Chemical Engineering, University of Waterloo, Waterloo, Canada. Email: dougla5@mcmaster.ca

Received: 05 June 2022, Revised and Accepted: 20 July 2022

ABSTRACT

Objective: The objective of this paper is to illustrate uses of Aspen Plus (Aspen) to pharmaceutical processes with a specific focus on the production of aspirin. Chemical process simulators such as Aspen have received little attention for pharmaceutical applications; this is due in part to prevalence of dynamic batch reactors, specialized raw materials and products often including solids and solids handling unit operations.

Methods: Aspen was used to first validate an experimental study and then extended to a commercial scale process.

Results: Aspen adequately reproduced the experimental results obtained from a dynamic batch reactor. Extension to the commercial scale illustrated the power of Aspen to simulate pharmaceutical processes as well as provide costing and economic analysis.

Conclusions: It was found that although the modeling of this relatively simple process is more complicated than it initially seemed, Aspen was capable of handling the difficulties inherent in dealing with solids, batch reactions, and crystal growth. In addition, its optimization and economic analysis features provided enhanced flow sheeting functionality. Its batch reactor model, RBATCH, is capable of modeling batch reactors involving multiple solid-liquid reactions following various reaction rate laws.

Keywords: Process simulation, Pharmaceuticals, Aspen Plus, Aspirin, Economic analysis.

 DOI: http://dx.doi.org/10.22159/ajpcr.2022v15i9.45749. Journal homepage: https://innovareacademics.in/journals/index.php/ajpcr

INTRODUCTION

Process simulation tools have been used successfully to model continuous processes in the chemical, petrochemical industries for decades but have not been adopted by the pharmaceutical industries with the same enthusiasm. The dynamic batch nature of pharmaceutical processes makes them more difficult to simulate than their large scale continuous cousins [1]. In addition, the frequent use of solids is also problematic for some process simulators.

Acetylsalicylic acid (ASA), commonly known as ASA or aspirin, is a well-known medicine used for fever, pain, and inflammation. Felix Hoffman, a chemist working with the Friedrich Bayer and Co., first synthesized ASA in 1897 and it was patented in 1899 as Aspirin [2]. Concern over its blood-thinning properties led doctors to become concerned that it may promote stomach ulcers and associated bleeding; as a result, coated-ASA was developed to dissolve slowly in the gut. However, these blood-thinning properties also provided new applications and it is now widely recommended by doctors for individuals who are at risk of a heart attack. In addition, it is recommended to immediately chew two 81 mg baby-aspirins if one is experiencing a heart attack. More recently, medical researchers have found that low doses of ASA may also protect against various cancers and perhaps Alzheimer's disease [2]. The US daily consumption of ASA was 80 million tablets or approximately 29 billion per year or 117 tablets per person per year [3].

The synthesis of ASA is based on the following overall chemical reaction:

Salicylic acid + acetic anhydride → acetylsalicylic acid + acetic acid

$C_7H_6O_3 + C_4H_6O_3 \rightarrow C_9H_8O_4 + C_2H_4O_2$

$SA + AA \rightarrow ASA + HA$

Joiner *et al*. [4] reported that the overall reaction, above, is actually comprised six elementary reactions that occur simultaneously but at different speeds. The kinetic rate laws for the elementary reactions are represented by following six differential equations. Note the large variation in the rate constants k, varying from 0.034 to 950 tending to make the system of differential equations stiff and more difficult to solve. Also note the appearance and subsequent disappearance of the intermediate species ASAA (acetylsalicylic anhydride).

$$SA(s) \rightarrow SA$$
$$\frac{d[SA]}{dt} = k_d\left([SA](T)^{sat} - [SA]\right)^d \quad k_d = 7.25, d = 1.90 \tag{1}$$

$$AA + SA \rightarrow ASA + HA$$
$$\frac{d[ASA]}{dt} = k_1[AA][SA]\, k_1 = 3.4\times10^{-2} \tag{2}$$

$$2ASA + AA \rightarrow ASAA + HA$$
$$\frac{d[ASAA]}{dt} = k_2[ASA]^2[AA]\, k_2 = 4.9\times10^{-1} \tag{3}$$

$$ASAA + H_2O \rightarrow 2ASA$$
$$\frac{d[ASA]}{dt} = k_3[ASA][H_2O]\, k_3 = 9.5\times10^{2} \tag{4}$$

$$AA + H_2O \rightarrow 2HA$$
$$\frac{d[HA]}{dt} = k_4[AA][H_2O]\, k_4 = 8.4\times10^{1} \tag{5}$$

$$ASA \rightarrow ASA(s)$$
$$\frac{d[ASA(s)]}{dt} = k_c\left([ASA] - [ASA](T)^{sat}\right)^c \quad k_c = 1.2, c = 1.34 \tag{6}$$

Joiner *et al*. [4] performed a relatively simple four-step experiment:

1. mix:
   - 9.5 g of salicylic acid powder, SA(s)
   - 20 ml of acetic anhydride liquid, AA
   - 0.2 ml of phosphoric acid (catalyst)
   - heat to 55°C and hold for 60 min while stirring
2. add 1 ml of water/min for 4 min
3. hold at 55°C for 56 min
4. cool down in 5 steps of 10°C each; hold for 24 min after each step (ASA(s) will begin to crystallize during this cooling step and therefore the concentration of dissolved ASA will begin to decrease).

Fig. 1 is a plot of the concentration of dissolved ASA as a function of time [4].

Initially, ASA was produced as a result of reactions (1, 2, and 3); then, reaction (3) takes over and consumes the already produced ASA to produce AASA (an intermediate product). Once the water is added the ASAA is very quickly converted back into ASA according to reaction (4). Once the cooling process starts ASA[s] begins to crystalize according to reaction (6) and the concentration of dissolved-ASA begins to decrease.

METHODS

The simulations performed in this research were all performed using Aspen Plus v11.2 [5].

Simulation of experimental results

The experimental results, shown in Fig. 1, were simulated using Aspen. When preparing to perform the simulation one needed to answer three key questions:

1. Are all the components available in the Aspen databanks?
2. Does Aspen have the appropriate thermodynamic model?
3. Does Aspen have the appropriate unit operation models?

Aspen has an extensive databank of more than 37,000 components including all components present listed in the six elementary reactions, with the exception of ASAA. If a component is present as a solid, then it needs to be specified as such. Aspen has an extensive library of thermodynamic models to choose from; for pharmaceutical processes, which generally operate at mild temperature and pressure conditions, Aspen recommends using the NRTL equation of state [5,6]. Finally, Aspen has a selection of rigorous reactor models employing both equilibrium and kinetic calculations including a dynamic batch reactor model, RBATCH, in which both equilibrium and kinetic calculations can be used.

To add a new component to Aspen's databank, one needs to either provide the pure component property information or provide the molecular structure and allow Aspen's built-in group contribution models to estimate the property values. The molecular structure can be provided either be using Aspen's drawing tool or by importing a so-called *MOL* file which is a text file that contains structure information; this method was found to be extremely straight forward [7].

The simplest way to simulate the experiment was to simulate each step using a separate batch reactor model. The resulting flow sheet is shown in Fig. 2, where the steps (1–4) are noted in or near each batch reactor model icon.

RESULTS AND DISCUSSION

Fig. 3 presents a comparison of (a) the experimental results [4] with (b) the Aspen predictions.

Fig. 3 shows that Aspen was able to reproduce the experimental results extremely well. The simulation was an ideal simulation of of the 4-step experimental recipe (above), while the experimental results include the effects of inherent experimental difficulties such as flow and temperature control and composition estimation/measurement.

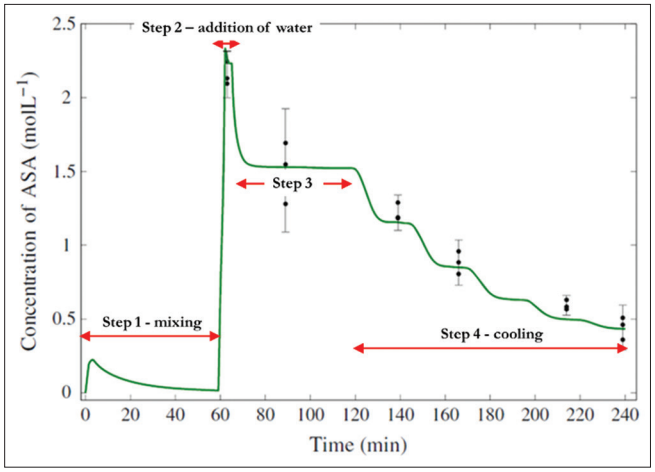

Fig. 1: Concentration of dissolved ASA as a function of time [4]

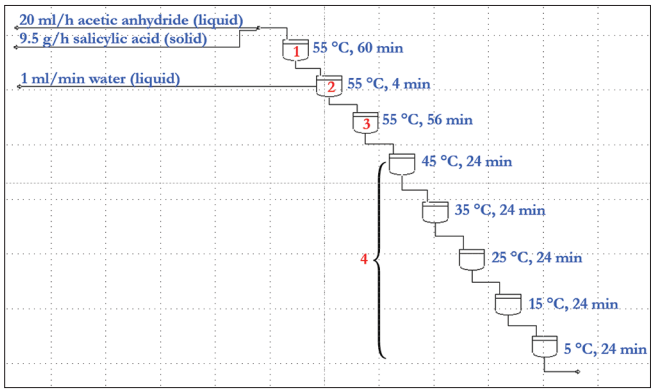

Fig. 2: Aspen simulation to mimic 4-step experiment [4]

Nevertheless, the excellent agreement is a strong indication of Aspen's abilities to model dynamic rate process of multiple reactions involving solids.

Continuous process to produce ASA

Based on Aspen's successful modeling of the experimental results, a preliminary flow sheet to represent a continuous process to produce ASA was developed. Fig. 4 is an overview of the continuous process showing the major sections in the process; note that each of the major sections contains several ancillary units such as pumps, blowers, heaters, and coolers. The overall proposed process contains three raw material feed streams (AA, solid-ASA, and Water) and two product streams (solid-ASA and Flue Gas). The raw material feeds to the process first enter the Batch Reactor section. The products from the Batch Reactor section leave the reactor and are fed to Crystallizer section which mimics the precipitation of solid-ASA by cooling. The solid-liquid stream containing solid-ASA is then fed to the Recrystallizer section to remove any dissolved impurities. The solid-ASA stream is fed to the Dryer section, where the remaining liquid is evaporated and the dry ASA product is collected. The waste streams from the Crystallizer, Recrystallizer, and Dryer Recrystallizer sections are sent to the Incinerator section to be destroyed, that is, converted into carbon dioxide and water and subsequently vented to the atmosphere.

The initial feed specifications were based on the 4-step experiment, in which 9.5 g of SA powder was mixed with 20 ml of AA. This feed mixture was subsequently adjusted (maintaining the mixture ratio) using a so-called Design-spec to ensure an overall production rate of 145 kg/h (1160 tonnes/y) of ASA solid product which is estimated to be the annual Canadian consumption.

Batch reactor section

The Batch Reactor section includes two batch reactors, modeled using Aspen's RBATCH model. The reaction stoichiometry, kinetic law, and rate constants for all six reactions (1–6) were entered. The SA enters the first reactor as a solid and the AA enters as a liquid. The reactors operate at 55°C, and all six reactions were *allowed* to take part in the reaction. Once the stopping criteria have been reached that the contents are transferred to the second reactor, where water is added. The RBATCH model calculates the composition as a function of time, as is shown in Fig. 5. Fig. 5a shows the dynamic interplay between reactions (1–3). Initially, solid SA, SA (s), dissolves into the liquid AA. Then, the SA in solution is consumed to produce ASA through reaction 2. Finally, the ASA is consumed to produce ASAA. The reactions are nearly complete after 10 min. In Fig. 5b one can see the rapid reaction (2.5 s) between H_2O and ASAA to produce ASA.

Crystallizer section

The crystallizer section is comprised of a crystallizer and centrifuge, modeled using Aspen's CRYSTALLIZER and CFUGE, respectively. The crystallizer section is designed to convert dissolved-ASA into solid-ASA by crystallization through cooling the solution below its solubility limit. The solubility of dissolved-ASA in the crystallizer feed stream was estimated by Aspen and is shown below in Fig. 6 over the temperature range 2–100°C.

As a point of comparison, the solubility of ASA in pure water at 20°C is only 3 g/l, however, the crystallizer feed stream contains almost

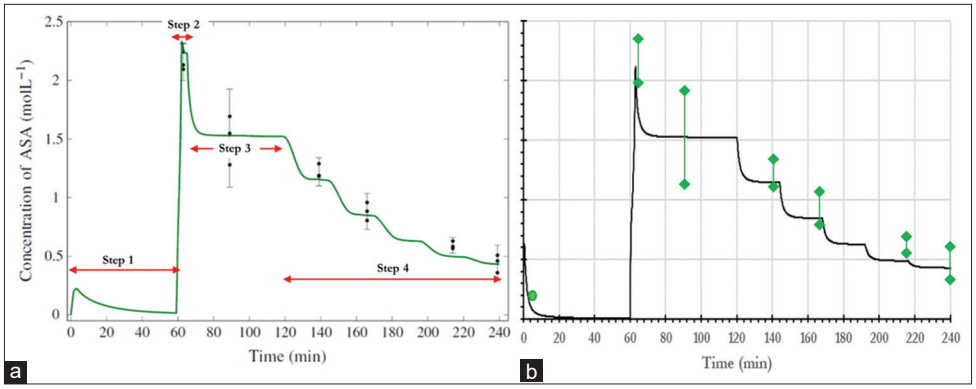

Fig. 3: Concentration of dissolved ASA as a function of time (a) experimental results [4] (b) Aspen predictions

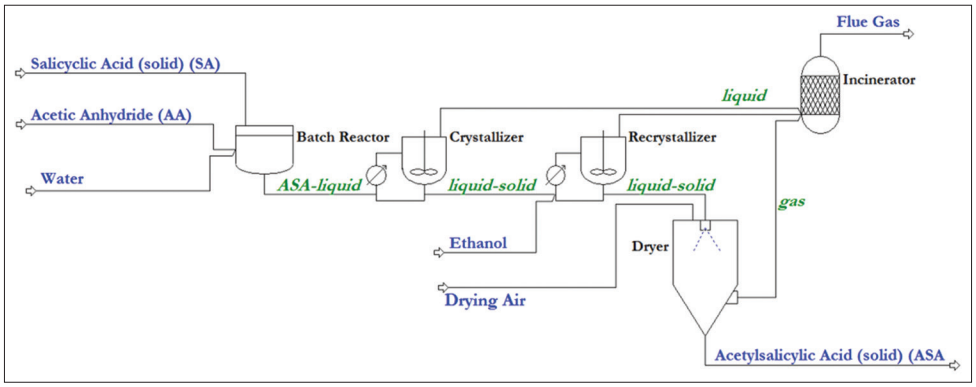

Fig. 4: Continuous process to produce ASA

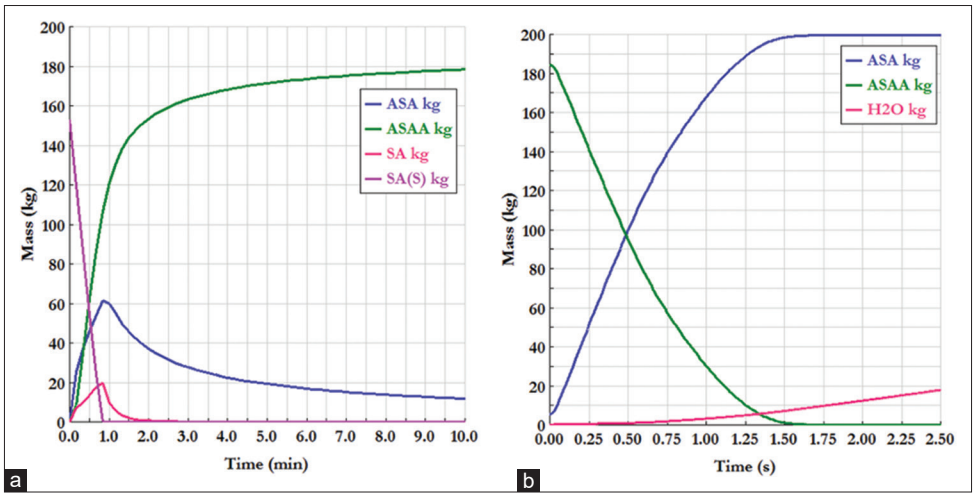

Fig. 5: Mass in reactor (a) after mixing SA powder + AA (prior to addition of H_2O) (b) after the addition of H_2O

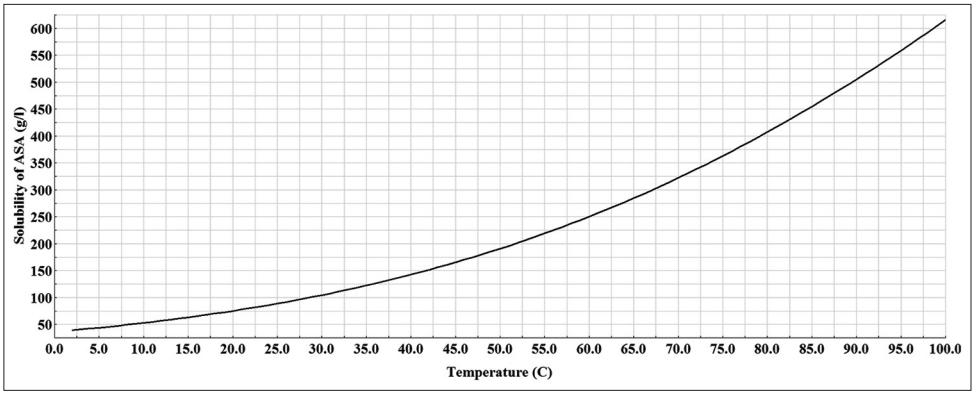

Fig. 6: Solubility of ASA in the crystallizer feed stream as a function of temperature

40 wt.% acetic acid which increases the solubility of ASA significantly. Once the temperature is cooled in the crystallizer, solid ASA begins to precipitate according to the solubility curve. While the operation of the crystallizer is conceptually simple and relatively easy to estimate the amount of solid crystallized, based on solubility curves, the complexity arises when one considers the crystal or particle size of the solid product. Predicting and controlling the crystal size has been the subject of many studies and is discussed below.

The solid-liquid stream leaving the crystallizer enters a centrifuge modeled using Aspen's CFUGE model. The centrifuge is designed to separate the solid-ASA from the solid-liquid stream by spinning the mixture at high velocity. The cyclone was designed to separate all of the solid-ASA from the solid-liquid stream, while allowing 15% of the supernatant liquid to remain with the solid stream (~ 17 wt.% moisture [dry basis]) which is typical in ASA dyers [8]. The temperature of both the solid and supernatant liquid streams is left at 3°C and the unit operation is isobaric.

Dryer section

The dryer section is comprised a blower and a dryer modeled using Aspen's COMPR and DRYER, respectively. Dry, ambient air, is blown at a slight positive pressure into the dryer, where it is heated to 40°C. The pressure is assumed to be atmospheric with an air-to-solid ratio of 15 kg air/kg ASA [8]. The dryer model produces two streams, a dry solid ASA stream and a vapor stream, which contains the now humidified drying air. The ASA stream is the final product stream containing 145 kg/h of ASA product. The vapor stream is sent to the incinerator section.

Incinerator section

The incinerator section is modeled using an RGIBBS reactor model to carry out a combustion reaction at equilibrium. The purpose of the incinerator is to safely dispose of all waste products by combusting them with natural gas (CH_4) at high temperature. The unit operates at atmospheric pressure and approximately 1034°C; typical biohazard incinerators operate at temperatures greater than or equal to 1000°C [9]. Natural gas was combusted with air in the presence of the waste streams, resulting in the production of mainly carbon dioxide and water which exit the incinerator. The RGIBBS model was set to operate adiabatically resulting in an Adiabatic Flame Temperature of 1034°C with a natural gas flow rate of 160.428 kg/h. However, at this high temperature, the Aspen cost estimation model failed, because the tensile strength of steel was now below a critical limit. As a "work-around," the operating temperature in the RGIBBS model was reduced to the maximum allowed temperature for costing purposes, which was found to be 500°C.

Heaters, coolers, pumps, and blowers

Multiple, heaters, coolers, pumps, and blowers were placed throughout the process for capital and utility costing purposes. Aspen does not actually require these models to perform the material and energy balance calculations, as temperature and pressure regulation are built into the unit operations.

Crystal size

As noted above, the prediction of crystal size is complex and has been the subject of many studies. Aspen predicts nucleation rate *B*, and crystal growth rate, *G*, as follows: [10].

$$B = k_b G^i M_t^j R^k \tag{7}$$

$$G = G_0\left(1+\gamma \bar{d}\right)^{\alpha} \tag{8}$$

$$k_b = 4 \times 10^{18} \tag{9}$$

$$i = 1.5 \tag{10}$$

$$j = 0.9 \tag{11}$$

$$k = 2.5 \tag{12}$$

$$\alpha = 0 \tag{13}$$

$$\gamma = 0 \tag{14}$$

Where:

B = crystal mass nucleation rate $\left(\frac{kg/m^3}{s}\right)$

G = crystal size growth rate $\left(\frac{m}{s}\right)$

G_0 =growth rate of a zero sized crystal $\left(\frac{m}{s}\right)$

M_t = magma density $\left(\frac{kg}{m^3}\right)$

$\bar{d}$ = mean crystal size (*m*)

R = impellor speed (*rpm*)

Using the default parameters, equations (10–14) lead to a predicted mean crystal size $\bar{d}$, of approximately $2.59\times 10^{-6} m$ (2.59 μm); however, the literature suggests that ASA crystals have a mean size of $\bar{d} \sim 125\mu m$ and a standard deviation of $\sigma \sim 25\mu m$ [11]. This, then, leads to a multi-objective parameter estimation problem, that is, what are the best values of the six unknown parameters, $\left(k_b, i, j, k, \alpha \text{ and } \gamma\right)$, to try and ensure that $\bar{d} \sim 125\mu m$ and $\sigma \sim 25\mu m$. The multi-objective optimization problem can be formulated as follows:

$$\min f_1(\boldsymbol{x}) = \left(\bar{d} - 125\right)^2$$

$$\min f_2(\boldsymbol{x}) = \left(\sigma - 25\right)^2$$

$$\boldsymbol{x} = \left\{k_b, i, j, k, \alpha, \gamma\right\}$$

$0 \le k_b \le 1 \times 10^{20}$

$-10 \le i \le 10$

$-10 \le j \le 10$

$-10 \le k \le 10$

$-10 \le \alpha \le 10$

$0 \le \gamma \le 1 \times 10^{20}$ (15)

Where the range of the unknown parameters is provided by Aspen. The multi-objective optimization problem (15) can be reformulated into a single-objective optimization problem as follows [12]:

$$\min_{k_b,i,j,k,\alpha,\gamma} \omega_1\left[\frac{f_1(x)-f_1^*}{f_1^N-f_1^*}\right]+\omega_2\left[\frac{f_2(x)-f_2^*}{f_2^N-f_2^*}\right]$$

$$\text{s.t} \sum \omega_1+\omega_2=1$$

$$0 \le k_b \le 1\times 10^{20}$$

$$-10 \le i \le 10$$

$$-10 \le j \le 10$$

$$-10 \le k \le 10$$

$$-10 \le \alpha \le 10$$

$$0 \le \gamma \le 1\times 10^{20} \quad (16)$$

Note that the two objectives have been normalized to account for magnitude and unit differences between the two objectives. Multiple optimizations will be required to account for various values of the weighting factor ω. The ideal solution is clearly the case when $\bar{d}=125\,\mu m$ and $\sigma=25\,\mu m$; this then corresponds to f_1^* = (125–125)^2 =0 and similarly f_2^* = (25–25)^2 =0 or $\left[f_1^*, f_2^*\right]=[0,0]$, while the worst case (the so-called *nadir,* ℕ) is $\left[f_1^N, f_2^N\right]$ where f_1^N is the value of $f_1(x)$ when $f_2(x)$ is minimized individually and f_2^N is value of $f_2(x)$ when $f_1(x)$ is minimized individually. To obtain f_1^N and f_2^N, one needs to perform two individual optimizations as follows. First start with f_2^N; consider the case when ω_1 = 1 and ω_2 = 0, problem (16) can be simplified as follows:

$$\min_{k_b,i,j,k,\alpha,\gamma}\left[\frac{f_1(x)-f_1^*}{f_1^N-f_1^*}\right]$$

Since $\left[f_1^*\right]=[0]$ at $\bar{d}=125\,\mu m$ we can write

$$\min_{k_b,i,j,k,\alpha,\gamma}\left[\frac{f_1(x)}{f_1^N}\right]$$

also since $\left[f_1^N\right]$ is not *yet* known, minimize $f_1(x)$ individually, that is,

$$\min_{k_b,i,j,k,\alpha,\gamma} f_1(x)=\left(\bar{d}-125\right)^2 \quad (17)$$

Once the minimum value of $f_1(x)$ has been found the corresponding value for f_2 which is f_2^N. In a similar fashion one can determine f_1^N.

Aspen has three built-in optimization solvers:
1. SQP (Sequential Quadratic Programming)
2. Complex (Box's Method)
3. BOBYQA.

Fig. 9 shows the predicted particle size distributions after solving problem (17) when ω_1 = 1. Clearly, the BOBYQA method is best since it is able to find a solution that reduces the value of the objective function to approximately 0, whereas the other two methods are unable to make significant reductions in the objective function. While it is not clear why the SQP and Complex methods fail to find the correct solution, it is of interest to note that the SQP method is based on quadratic programming (QP) and both Complex and BOBYQA are direct search methods which do not use gradient information. The objective function in problem (17) is quadratic, which should lend itself to SQP; however, the equality constraints (7 and 8) are both very non-linear and need to be linearized to transform the problem into a QP.

Fig. 8 shows the normalized Pareto front along with the objective function from problem (16). The normalized point (0, 1) corresponds to the problem when ω_1 = 1 and the point (1, 0) corresponds to the ω_2 = 1.

Economic analysis

Aspen also has the ability to estimate the cost of the various unit operations as well as perform an economic analysis of the process. Cost estimation in general and the Aspen Economic Analysis sub-section in particular is rather complex. Therefore, as this is a preliminary study, the default Aspen settings were used with the exception of materials of construction; stainless steel (316SS) was specified for this pharmaceutical process. A summary of the results is presented in Fig. 9.

It is clear from Fig. 9 that the major economic items are the raw material costs and product revenues, while capital and operating/utility costs are insignificant. Although the cost estimates are extremely preliminary and do not include costs related to raw material preparation, tablet preparation and packaging, R&D costs, etc., the difference between the estimated costs of production and sales illustrates the potentially high profit margins enjoyed by the pharmaceutical industry.

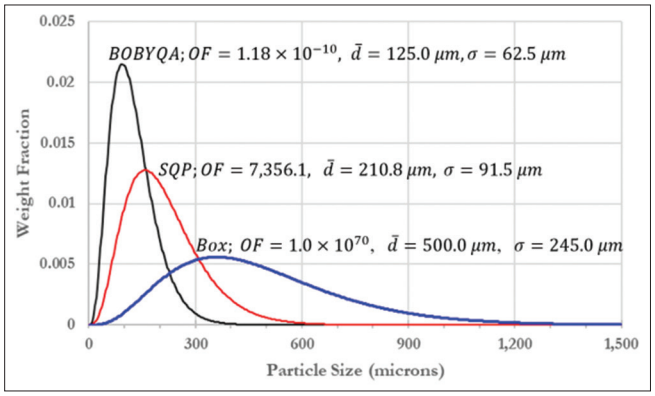

Fig. 7: Particle size distributions after optimization of problem (17), (ω_1 = 1)

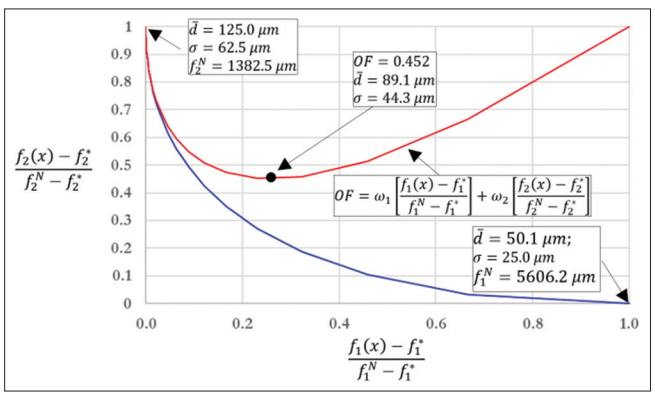

Fig. 8: Normalized Pareto front and optimization of problem (16)

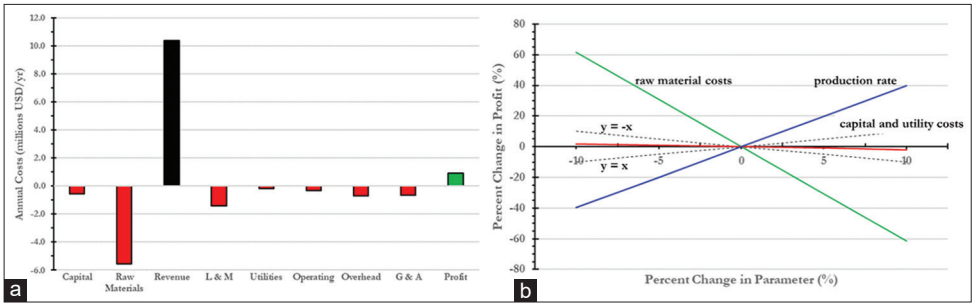

Fig. 9: Economic analysis results (a) annual costs (b) sensitivity of profit to changes in parameter costs

CONCLUSIONS

Based on this preliminary technoeconomic analysis of an ASA process using Aspen, the following conclusions can be reached.

1. Modeling of this relatively simple process is more complicated than it initially seemed, based on experiments. This is due largely to the process' multiple reactions with significantly different reaction rates and both dissolution and crystallization of solids.
2. Aspen is a comprehensive and powerful simulation system and is an appropriate tool for modeling pharmaceutical processes. Its RBATCH reactor model is capable of modeling batch reactors involving multiple solid-liquid reactions following various reaction rate laws.
3. Following a preliminary economic analysis, the profit was found to be *insensitive* to changes or errors in capital and utility costs and *sensitive* to changes in raw material costs and production rate. Therefore, future work should focus on reducing raw material costs and/or increasing capacity as incentives for advanced control and optimization studies are likely small.

ACKNOWLEDGMENT

Declared none.

AUTHORS' CONTRIBUTIONS

Ali Elkamel provided the idea and motivation for the study as well as checking results and proofing the manuscript. Alisa Douglas performed the simulations and manuscript drafting.

CONFLICTS OF INTEREST

Declared none.

FUNDING SOURCES

The authors acknowledge funding from the Natural Sciences and Engineering Research Council of Canada (NSERC) and Magnet for the support of Alisa Douglas during her co-op work term.

REFERENCES

1. Petrides DP, Koulouris A, Lagonikos PT. The role of process simulation in pharmaceutical process development and product commercialization. Pharm Eng 2002;22:1-4.
2. Connelly D. A History of Aspirin; 2014. Available from: https://pharmaceutical-journal.com/article/infographics/a-history-of-aspirin [Last accessed on 2022 Jun 27].
3. Squires S. Aspirin: The World's most Popular Pill Turns 100. The Washington Post, WP Company; 1997. Available from: https://www.washingtonpost.com/archive/lifestyle/wellness/1997/08/05/aspirin-the-worlds-most-popular-pill-turns-100/caa961d1-c7a4-42c7-b1ac-550193a9a21f/last [Last accessed on 2022 Jun 27].
4. Joiner DE, Billeter J, McNally ME, Hoffman RM, Gemperline PJ. Comprehensive kinetic model for the dissolution, reaction and crystallization processes involved in the synthesis of aspirin. J Chemometrics 2014;28:420-8. doi: 10.1002/cem.2605.
5. Aspen Technology, Inc., 20 Crosby Drive, Bedford, Massachusetts 01730 USA; 2022. Available from: https://www.aspentech.com/en [Last accessed on 2022 Aug 05].
6. Al-Malah KI. Optimization of drug solubility using aspen plus: Acetylsalicylic acid (aspirin) solubility a second case study. Asian J Pharm Clin Res 2020;13:178-84. doi: 10.22159/ajpcr.2020.v13i4.37143.
7. National Library of Medicine. Acetylsalicylic Anhydride. Bethesda, Maryland: National Library of Medicine; 2022.
8. Pakowski Z, Mujumdar AS. Drying of Pharmaceutical Products; 2007. Available from: https://www.researchgate.net/publication/265314817_Drying_of_Pharmaceutical_Productslast [Last accessed on 2020 Aug 04].
9. Eberhartinger S. Draft Guidelines on BAT and BEP Medical Waste Incineration; 2004. Available from: http://chm.pops.int/Portals/0/docs/from_old_website/documents/meetings/bat_bep/2nd_session/egb2_followup/draftguide/5A2medicalwasteincinerationdraftb.pdf [Last accessed on 2022 Jun 28].
10. Bennett RC. Crystallization from solution. In: Perry's Chemical Engineers' Handbook. 6th ed. New York: McGraw-Hill; 1984. p. 24-40.
11. Mujumdar AS, editor. Handbook of Industrial Drying. 4th ed. Boca Raton, Florida: CRC Press; 2014.
12. Rangaiah GP, editor. Multi-objective Optimization Techniques and Applications in Chemical Engineering. Singapore: World Scientific Publishing, Pvt. Ltd.; 2009.